Korean J. Chem. Eng., **30**(4), 918-924 (2013)
DOI: 10.1007/s11814-012-0217-7

Chiral adsorption of phenylalanine by α-, β-cyclodextrin modified layered double hydroxides

Xiaolei Liu† and Lili Meng

Chemical Engineering Department, Zibo Vocational Institute, Zibo 255314, P. R. China
(*Received 2 August 2012 • accepted 16 December 2012*)

Abstract–The chiral adsorption of racemic phenylalanine (Phe) by carboxymethyl-α/β-cyclodextrin-intercalated Zn-Al layered double hydroxides (CM-α/β-CD-LDHs) has been studied. The adsorption isotherms of chiral excess adsorption and the total adsorption of Phe by these CM-α/β-CD-LDHs have been investigated. CM--CD-LDHs were found to be more suitable for chiral recognition of Phe than CM--CD-LDHs. Furthermore, the intraparticle diffusion model is successfully validated in this work. Intraparticle effective diffusivities (D_{eff}) of Phe in these CM-α/β-CD-LDHs macroparticles were determined from the homogeneous Fickian diffusion model at various temperatures.

Key words: LDHs, Adsorption, Parallel Diffusion, Phenylalanine, Chiral

INTRODUCTION

Efficient methodologies for the production of enantiomerically pure or enriched compounds are of great academic and industrial importance. Cyclodextrins (CDs) are widely utilized in studies of chiral and molecular recognition. CDs are cyclic (α-1,4)-linked oligosaccharides composed of α-D-glucopiranose. Those CDs consisting of six, seven, or eight glucose entities are called α-, β-, or γ-CD. CDs assume a toroidal shape with the primary hydroxyl groups at the narrow side and the secondary hydroxyl groups at the wide side. Their chemical structure presents a hydrophobic cavity that can encapsulate various guest molecules to produce supramolecular inclusion complexes, making them ideal prototypes for examining intermolecular interactions associated with molecular and chiral recognition [1-4]. The versatility of these macrocycles is remarkable, and they are extensively used in chiral chromatography due to their price-to-performance ratio. Both native and derivative CDs have been used to separate enantiomers in chromatography [5,6], and more recently, they were used as additives that enantioselectively bind and control the migratory aptitudes of analyses in capillary electrophoresis [7].

Layered double hydroxides (LDHs) are a class of layered materials consisting of positively charged brucite-like layers and exchangeable interlayer anions. LDHs can be represented by the general formula $[M^{II}_{1-x}M^{III}_{x}(OH)_2]^{x+}(A^{n-})_{x/n}\cdot mH_2O$ [8,9], where M^{II} and M^{III} are di- and trivalent metal cations, respectively. LDHs have positively charged layers and a wide variety of charge-balancing anionic species (A^{n-}). Numerous researches have shown that LDHs have a wide range of applications, such as catalyst precursors, ion exchangers, adsorbents for environmental contaminants and substrates for the immobilization of biological materials [10-12].

Recently, the intercalations of CDs with layered supports have attracted much attention. Modified CDs have been used as a "guest" molecule incorporated into layered hosts such as α-zirconium phosphate [13], montmorillonite [14], and layered double hydroxides [15,16]. In our previous work, the intercalation of carboxymethyl-β-CD into LDHs as well as the chiral adsorption of 1-phenyl-1,2-ethanediol (PED) was studied. Furthermore, the adsorption isotherms of chiral excess adsorption and the total adsorption of PED by CM-β-CD-LDHs powder and film have been studied by using the batch method. The parallel diffusion model was successfully used in this adsorption process [17,18].

In this paper, the carboxymethyl modified α-cyclodextrin and β-cyclodextrin were intercalated into the interlayer of LDHs. Furthermore, the chiral recognition of racemic phenylalanine (Phe) by these CM-α/β-CD-LDHs was investigated by using the batch method. L-Phe is a valuable chemical product that is widely used in food, animal feed-stock and pharmaceutical industries and is one of the eight essential amino acids. Compared with other methods used for chiral separation of Phe [19], CMCD-LDHs are easy and inexpensive to prepare and are environmentally friendly. The intraparticle diffusion model [20,21] was successfully validated in this work. Diffusivities (D) of Phe in these CMCD-LDHs were determined from the Fickian diffusion model. Compared with the chiral adsorption by CM-β-CD-LDHs, the CM-α-CD-LDHs shows higher chiral excess adsorption ratio, which was explained assuming that α-CD is much better suited to accommodate benzene derivatives than β-CD.

DIFFUSION MODEL

LDHs macroparticles are considered as agglomerates of spherical crystallites, which consist of LDHs layers and anions between the sheets. Moreover, there are many pores between the crystallites. The adsorbate molecules diffuse into pores and are adsorbed on the crystallites' walls, and then diffuse into the interlayer of LDHs crystallites. To simplify calculation, the LDHs crystallites are considered as microspheres, which can adsorb Phe at the surface. Meanwhile, Phe molecules can diffuse from one adsorption site to the next adsorption site, and also diffuse between the nearby crystallites. The macroparticles of LDHs are made up of many of these crystallite microspheres.

†To whom correspondence should be addressed.
E-mail: lxl5233@163.com

In this experimental study, the intraparticle diffusion of Phe in CM-α-CD-LDHs and CM-β-CD-LDHs was analyzed based on a parallel transport by Phe diffused in the crystallites (hereafter called crystallite diffusion) and the liquid-phase diffusion inside the network structure between crystallites (hereafter called pore diffusion). The following assumptions apply:

(1) Crystallite and pore diffusion occur in parallel inside the CMCD-LDHs macroparticles.

(2) Crystallite and pore diffusivities are constant throughout the adsorption process.

(3) The void fraction of CMCD-LDHs macroparticles is constant throughout the adsorption process.

(4) The bulk phase concentration of Phe is constant during the adsorption process.

The parallel diffusion model for this system can be written as follows:

$$\varepsilon\frac{\partial C}{\partial t}+(1-\varepsilon)\frac{\partial q}{\partial t}=D_p\varepsilon\frac{1}{r^2}\frac{\partial}{\partial r}\left(r^2\frac{\partial C}{\partial r}\right)+D_c(1-\varepsilon)\frac{1}{r^2}\frac{\partial}{\partial r}\left(r^2\frac{\partial q}{\partial r}\right) \tag{1}$$

Where C (mol/m^3) represents liquid-phase concentration of Phe inside the macroparticles and q (mol/m^3 wet LDHs) corresponds to solid-phase concentration of Phe on the surface of the crystallites microspheres. r (m) means radial dimension of an adsorbent particle. The symbol ε denotes the void ratio of LDHs macroparticles. D_c and D_p (m^2/s) are the effective diffusivities in the crystallites and in the pores, respectively. Using the dimensionless variables, Eq. (1) is transformed into Eq. (2):

$$\frac{\partial X}{\partial \tau_p}+\alpha\frac{\partial Y}{\partial \tau_p}=\frac{1}{\xi^2}\frac{\partial}{\partial\xi}\left(\xi^2\frac{\partial X}{\partial\xi}\right)+\beta\frac{1}{\xi^2}\frac{\partial}{\partial\xi}\left(\xi^2\frac{\partial Y}{\partial\xi}\right) \tag{2}$$

Where $X=C/C_e$, $Y=q/q_e$, $\tau_p=D_pt/r_0^2$, $\xi=r/r_0$, $\alpha=((1-\varepsilon)q_e)/\varepsilon C_e$, $\beta=((1-\varepsilon)q_eD_c)/\varepsilon C_eD_p=\alpha(D_c/D_p)$, and q_e (mol/m^3 wet LDHs) is the concentration of Phe on the adsorption sites, in equilibrium with the concentration of Phe in the bulk solution C_e (mol/m^3). r_0 (m) is radius of an adsorbent particle. The first and second terms of the right-hand side of Eq. (2) represent the contributions of pore diffusion and crystallite diffusion, respectively.

In this parallel diffusion model, α and β are the most important parameters. According to the definition, α means a distribution coefficient, while β is the ratio of the rate of crystallite diffusion to that of pore diffusion. The degree of the contributions of crystallite and pore diffusion should be evaluated from the value of β. There are two limiting cases to consider here: when $\beta\rightarrow 0$ ($\varepsilon D_pC_e>>(1-\varepsilon)D_cq_e$, pores diffusion controls) and when $\beta\rightarrow 0$ ($\varepsilon D_pC_e<<(1-\varepsilon)D_cq_e$; crystallite diffusion controls).

Equilibrium as described by the equilibrium isotherms holds at the interface between the liquid and solid phases. In this case, the model uses the Freundlich isotherm (Eq. (3)):

$$q=kC^{1/n} \tag{3}$$

Using the dimensionless variables, Eq. (3) is transformed into Eq. (4)

$$Y=k'X^{1/n} \qquad \left(k'=\frac{kC_e^{1/n}}{q_e}\right) \tag{4}$$

Using Eq. (4), Eq. (2) is transformed into Eq. (5), as follows:

$$\left\{\alpha+\frac{nY^{n-1}}{k'^n}\right\}\frac{\partial Y}{\partial\tau_p}=\frac{1}{\xi^2}\frac{\partial}{\partial\xi}\left(\xi^2\frac{nY^{n-1}}{k'^n}\frac{\partial Y}{\partial\xi}\right)+\frac{\beta}{\xi^2}\frac{\partial}{\partial\xi}\left(\xi^2\frac{\partial Y}{\partial\xi}\right) \tag{5}$$

In addition, the following initial and boundary conditions apply

$$\text{(I.C.) } X=0\ Y=0 \text{ at } \tau_p=0 \text{ or } \tau_c=0 \tag{6}$$

$$\text{(B.C.) } \frac{\partial X}{\partial\xi}=0\quad\frac{\partial Y}{\partial\xi}=0 \text{ at } \xi=0$$

$$X=1\ Y=1 \text{ at } \xi=1 \tag{7}$$

The current total concentration of Phe in the particle Q_t (mol/m^3 wet LDHs) in Eq. (8) can be determined with time, while equilibrium adsorption capacity Q_e (mol/m^3 wet LDHs) in Eq. (9) can be obtained by adsorption at enough time.

$$Q_t=(1-\varepsilon)q+\varepsilon C=\frac{V(C_{a,0}-C_{a,t})}{V_{LDHs}} \tag{8}$$

$$Q_e=(1-\varepsilon)q_e+\varepsilon C_e=\frac{V(C_{a,0}-C_{a,e})}{V_{LDHs}} \tag{9}$$

Where V and V_{LDHs} represent the solution volume and the wet LDHs volume. $C_{a,0}$, $C_{a,t}$ and $C_{a,e}$ represent the aqueous-phase Phe concentration at initial, at time t and at equilibrium, respectively.

Finally, the solution to the fractional attainment (F) of equilibrium under the initial and boundary conditions in Eq. (6) and Eq. (7), is given by Eq. (10):

$$F=\frac{Q_t}{Q_e}=\frac{3\int_0^{r_0}Q_tr^2dr}{r_0^3Q_e}=\frac{3\left[\alpha\int_0^1Y\xi^2d\xi+\int_0^1X\xi^2d\xi\right]}{\alpha+1}$$

$$=1-\sum_{n=1}^{\infty}\frac{6\omega(\omega+1)\exp(-D_{eff}\lambda_n^2t/r^2)}{9+9\omega+\lambda_n^2\omega^2} \tag{10}$$

Where the parameter D_{eff} represents the intraparticle effective diffusivity, and the λ_n values are the nonzero roots of

$$\tan\lambda_n=\frac{3\lambda_n}{3+\omega\lambda_n^2} \tag{11}$$

The parameter ω is expressed in terms of the final fractional uptake of solute by the LDHs macroparticles by the relation:

$$\frac{V_{LDHs}Q_e}{VC_{a,0}}=\frac{1}{1+\omega} \tag{12}$$

EXPERIMENTAL SECTION

1. Reagents

All chemicals including $Zn(NO_3)_2\cdot 6H_2O$, $Al(NO_3)_3\cdot 9H_2O$, NaOH, $NaNO_3$, methanol, chloroactic acid, α-cyclodextrin, β-cyclodextrin and (*L*, *D*)-phenylalanine were of analytical grade. They were purchased from the Beijing Chemical Plant Limited.

2. Preparation and Characterization

2-1. Synthesis of Carboxymethyl-α-cyclodextrin, CM-α-CD (3.7)

CM-α-CD was synthesized according to the procedure described in the literature [22] with some modifications. In brief, α-CD (29.3 g) and NaOH (35.2 g) were dissolved in 200 ml of water, and monochloroacetic acid (37.8 g) was added with gentle stirring. The mixture was heated at 80 °C for 3 h. The solution was then cooled in

an ice bath and the pH was adjusted to 6.0 with concentrated hydrochloric acid. Methanol was gradually added into the solution with stirring to obtain CM-α-CD precipitation. The average number of carboxylate groups (3.7) per CM-α-CD was calculated using ^{1}H NMR [23].

2-2. Synthesis of Carboxymethyl-β-cyclodextrin, CM-β-CD (4.1)

CM-β-CD was similarly synthesized as CM-α-CD. In brief, β-CD (34.4 g) and NaOH (35.2 g) were dissolved in 200 ml of water, and monochloroacetic acid (37.8 g) was added with gentle stirring. The mixture was heated at 80 ℃ for 3 h. The solution was then cooled in an ice bath and the pH was adjusted to 6.0 with concentrated hydrochloric acid. Methanol was gradually added into the solution with stirring to obtain CM-β-CD precipitation. The average number of carboxylate groups (4.1) per CM-β-CD was calculated using ^{1}H NMR.

2-3. Synthesis of CM-α/β-CD-LDHs

The precursor NO_3-LDH was prepared by a coprecipitation method similar to that reported previously [17]. A solution of $Zn(NO_3)_2$ (0.12 mol) and $Al(NO_3)_3$ (0.06 mol) in deionized water (200 ml) was added dropwise over 2 h to a solution of NaOH (0.31 mol) and $NaNO_3$ (0.21 mol) in water (100 ml). The white precipitate obtained was collected by centrifugation, washed thoroughly, and stored to be used later in an anion-exchange reaction. CM-α-CD-LDHs or CM-β-CD-LDHs were obtained by ion exchange. A solution of CM-α-CD (2.3 g) or CM-β-CD (2.5 g) in deionized water (50 ml) was added to a suspension of NO_3-LDHs (10.0 g) in water (100 ml) and the pH of the solution was kept at 6.0 by adding 0.1 mol/L NaOH solution or 0.1 mol/L HNO_3 solutions during the reaction. The mixtures were heated at 60 ℃ under a nitrogen atmosphere for 48 h. The products were washed extensively with deionized water, centrifuged, and dried at 70 ℃ for 20 h.

As Ca^{2+} cannot be adsorbed on LDHs layers, the void fraction of the CM-α/β-CD-LDHs, ε, was obtained by dissolving the CM-α/β-CD-LDHs whose pores were filled with $CaCl_2$ solution in HCl solution (1.0×10^2 mol/m^3). The concentration of Ca^{2+} in the filtrate was determined by ICP. The value of ε was calculated according to Eq. (13), where C_{Ca} is the concentration of Ca^{2+} filled in the pores (mol/m^3); W and θ are the weight of the wet CMCD-LDHs particles (kg) and the apparent density (kg of wet CMCD-LDHs m^{-3}), respectively; $C_{f,Ca}$ and V_f are the concentration of Ca^{2+} in the filtrate (mol/m^3) and the volume of the filtrate (m^3), respectively. The experimental physical properties of CM-α/β-CD-LDHs are listed in Table 1.

$$\varepsilon=\frac{C_{f,Ca}V_f}{(W/\theta)C_{Ca}} \quad (13)$$

3. Adsorption Experiments

Racemic Phe sorption experiments were carried out using the batch method. Both the effects of contact time and Phe concentration on the adsorption were investigated. The effect of contact time was used to determine a kinetic model of racemic Phe sorption and the equilibrium isotherm. In these experiments, the racemic Phe solutions were prepared with deionized water and racemic Phe of analytical purity. 3.0×10^{-4} kg of CM-α-CD-LDHs or CM-β-CD-LDHs and 2.0×10^{-5} m^3 of racemic Phe solutions (typically ranging from 0.0 to 90.9 mol/m^3) were added to 5.0×10^{-5} m^{-3} Erlenmeyer stopper flasks. After being capped and vigorously shaken by hand, the flasks were placed in a water bath at certain temperature (e.g., 303 and 323 K) and gently shaken for specific time period or until adsorption equilibrium. The suspensions were filtered, and the racemic Phe concentrations were determined using UV-vis spectrophotometer at λ=258 nm. The amount of racemic Phe adsorbed by the CM-α/β-CD-LDHs was calculated by the difference between the initial ($C_{a,0}$) and equilibrium concentrations ($C_{a,e}$), per kilogram of CM-α/β-CD-LDHs adsorbent: $Q_{total}=(C_{a,0}-C_{a,e})\times V/m$.

4. Characterization

Powder X-ray diffraction (XRD) patterns of the samples were recorded using a Shimadzu XRD-6000 diffractometer with Cu-Kα radiation (λ=1.5406 Å). The operating voltage and current were 40 kV and 30 mA, respectively. The step used was 0.02° s^{-1} in the 2θ range from 3 to 70°. Metal analysis was performed by ICP emission spectroscopy on a Shimadzu ICPS-7500 instrument using solutions prepared by dissolving the samples in dilute HCl. The concentration of Phe in the solutions, before and after adsorption experiments, was determined by the UV-vis spectra at the wavelength of 258 nm. Optical rotations were measured with a Jasco DIP-1000 digital polarimeter, which was used to determine e.e.% of the solutions after the adsorption experiment.

RESULTS AND DISCUSSION

1. Characterization of CM-α/β-CD-LDHs

The XRD patterns of NO_3-LDH, CM-α-CD-LDHs and CM-β-CD-LDHs are displayed in Fig. 1, and the lattice parameters are listed in Table 2. All the patterns indicate formation of well-crystallized hydrotalcite-like LDHs phase. In each case, the reflections can be indexed to a hexagonal lattice with *R*-3m rhombohedral symmetry, commonly used for the description of LDHs structures. However, as is often the case, several of the (*hkl*) reflections (b, c) disappear or broaden compared with those of the precursor NO_3-LDH (a). The value of the lattice parameter, *a*, which can be calculated as $a=2d_{110}$, is a function of the average distance between the metal ions, and thus, since Al^{3+} is smaller than Zn^{2+}, gives an indication of the Zn^{2+}/Al^{3+} ratio. For our materials, the values of *a* for the samples are very similar, indicating that there is no significant difference in Zn^{2+}/Al^{3+} ratio. In contrast, the values of the lattice parameter *c* for the samples are quite different. The value of *c* is related to several

Table 1. Experimental physical properties of CMCD-LDHs

	CM-α-CD-LDHs	CM-β-CD-LDHs
Particle diameter (m)	2.01×10^{-4}	1.97×10^{-4}
True density (kg of dry CMCD-LDHs m^{-3})	1.86×10^3	1.89×10^3
Apparent density (kg of wet CMCD-LDHs m^{-3})	1.19×10^3	1.17×10^3
The void fraction of CMCD-LDHs macroparticles	0.346	0.332

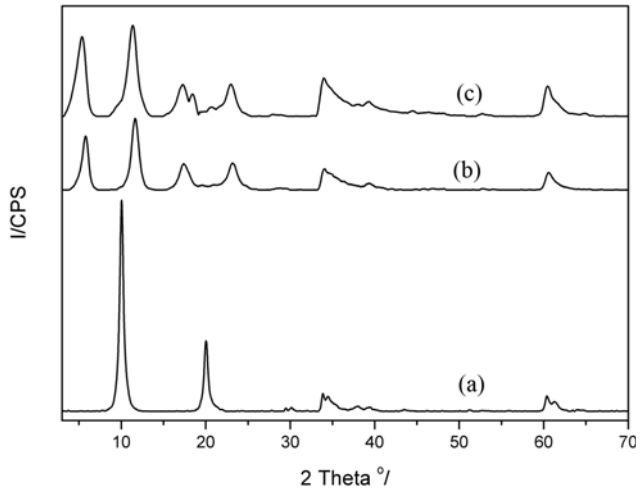

Fig. 1. XRD patterns of (a) NO_3-LDHs, (b) CM-α-CD-LDHs, (c) CM-β-CD-LDHs.

Table 2. Lattice parameters of NO_3-LDHs and CMCD-LDHs

Lattice parameter (nm)	NO_3-LDHs	CM-α-CD-LDHs	CM-β-CD-LDHs
d_{003}	0.889	1.523	1.647
d_{006}	0.445	0.758	0.780
d_{009}	0.297	0. 510	0.514
d_{110}	0.152	0.152	0.152
Lattice parameter *a*	0.304	0.304	0.304
Lattie parameter *c*	2.667	4.569	4.941

factors such as the anion size, orientation, and extent of hydration.

The intercalation of CM-α/β-CD in the lamellar host structure was clearly evidenced by the increase in the basal spacing d_{003} from 0.889 nm for the precursor NO_3-LDHs to 1.523 nm for CM-α-CD-LDHs and 1.647 nm for CM-β-CD-LDHs. The corresponding gallery heights were calculated to be 0.409, 1.043 and 1.167 nm, respectively, by subtracting the thickness of the inorganic layer (0.48 nm) [18]. Taking into account the dimensions of the carboxymethyl modified cyclodextrin molecule (CDs should be regarded as a truncated cone with the height of CM-α/β-CD is 1.06 nm [17]), CM-α/β-CD must both adopt a monolayer arrangement with its cavity axis perpendicular to the LDHs layer and carboxymethyl groups on the narrow sides of the cyclodextrin cavity attached to the LDHs surface.

2. Chiral Adsorption

The optical rotations of the solution were measured to determine the e.e.%. The results indicate that *L*-Phe was adsorbed preferentially both by CM-α-CD-LDHs and CM-β-CD-LDHs. The excess adsorption of L-Phe over D-Phe (Q_{ce}) resulting from the chiral reorganization of interlayer immobilized CM-α/β-CD and the total adsorption can be calculated by

$$Q_{ce}=C_{a,t}\times V\times e.e.\%/m \quad (14)$$

$$Q_{total}=(C_{a,0}-C_{a,t})\times V/m \quad (15)$$

Thus the adsorption isotherms, including chiral excess adsorption and the total adsorption, were plotted and shown in Fig. 2.

In these figures, both the CM-α-CD-LDHs and CM-β-CD-LDHs

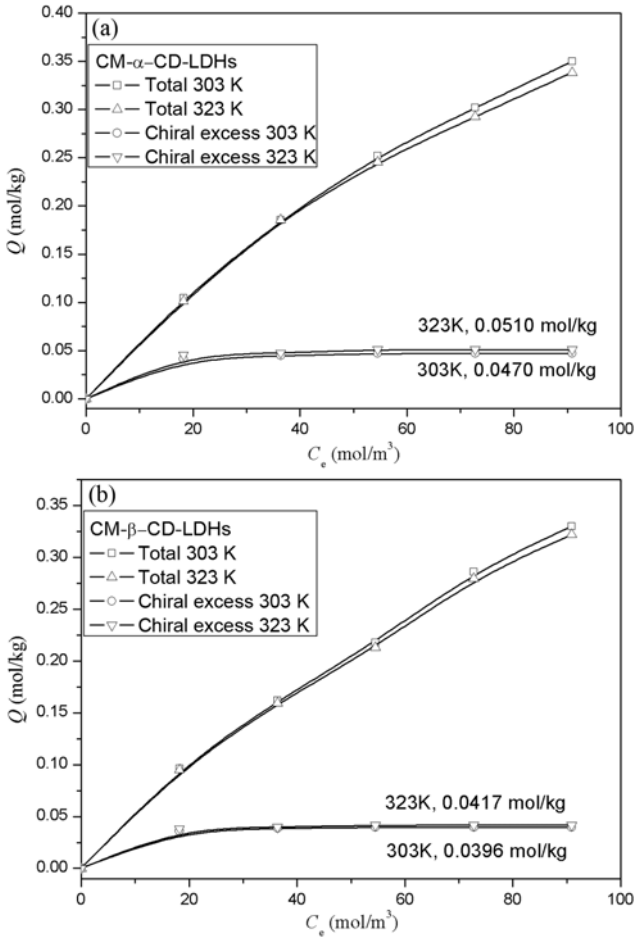

Fig. 2. The total and chiral excess adsorption isotherms of Phe by (A) CM-α-CD-LDHs, (B) CM-β-CD-LDHs at 303 K and 323 K.

can be used to enantioselectively adsorb Phe. According to the classification of IUPAC, the shape of its enantioselective isotherm can be considered as Type I. The chiral excess adsorptions by CM-α-CD-LDHs and CM-β-CD-LDHs have a maximum adsorption capacity (CM-α-CD-LDHs at 303 K $Q_{ce,e}$=0.0470 mol/kg, at 323 K $Q_{ce,e}$= 0.0510 mol/kg, and CM-β-CD-LDHs at 303 K $Q_{ce,e}$=0.0396 mol/kg, at 323 K $Q_{ce,e}$=0.0417 mol/kg,). Moreover, in all the adsorption, the amount of chiral excess adsorption increases with the increase of temperature. The explanation for this behavior is that the chiral excess adsorption is caused by the chiral inclusion of CDs accommodated in the interlayer region of LDHs, which is an energy-needed process, so higher temperature is beneficial to chiral adsorption. Owing to the shape of the isotherms, the total sorption data were analyzed based on Freundlich equation.

Interestingly, the chiral excess adsorptions of CM-α-CD-LDHs (0.0470 mol/kg at 303 K and 0.0510 mol/kg and 323 K) are significantly higher than that of CM-β-CD-LDHs (0.0396 mol/kg at 303 K and 0.0417 mol/kg and 323 K). It can be explained that the radius of the α-CD cavity is 0.42 nm as measured in the O4 hexagon. This cavity size is most suitable for the inclusion of a benzene ring with its long axis parallel to the molecular axis of α-CD cavities, if we consider van der Waals radii. Therefore, a Phe molecule can be fully included in the α-CD cavities and can be more enantioselectively

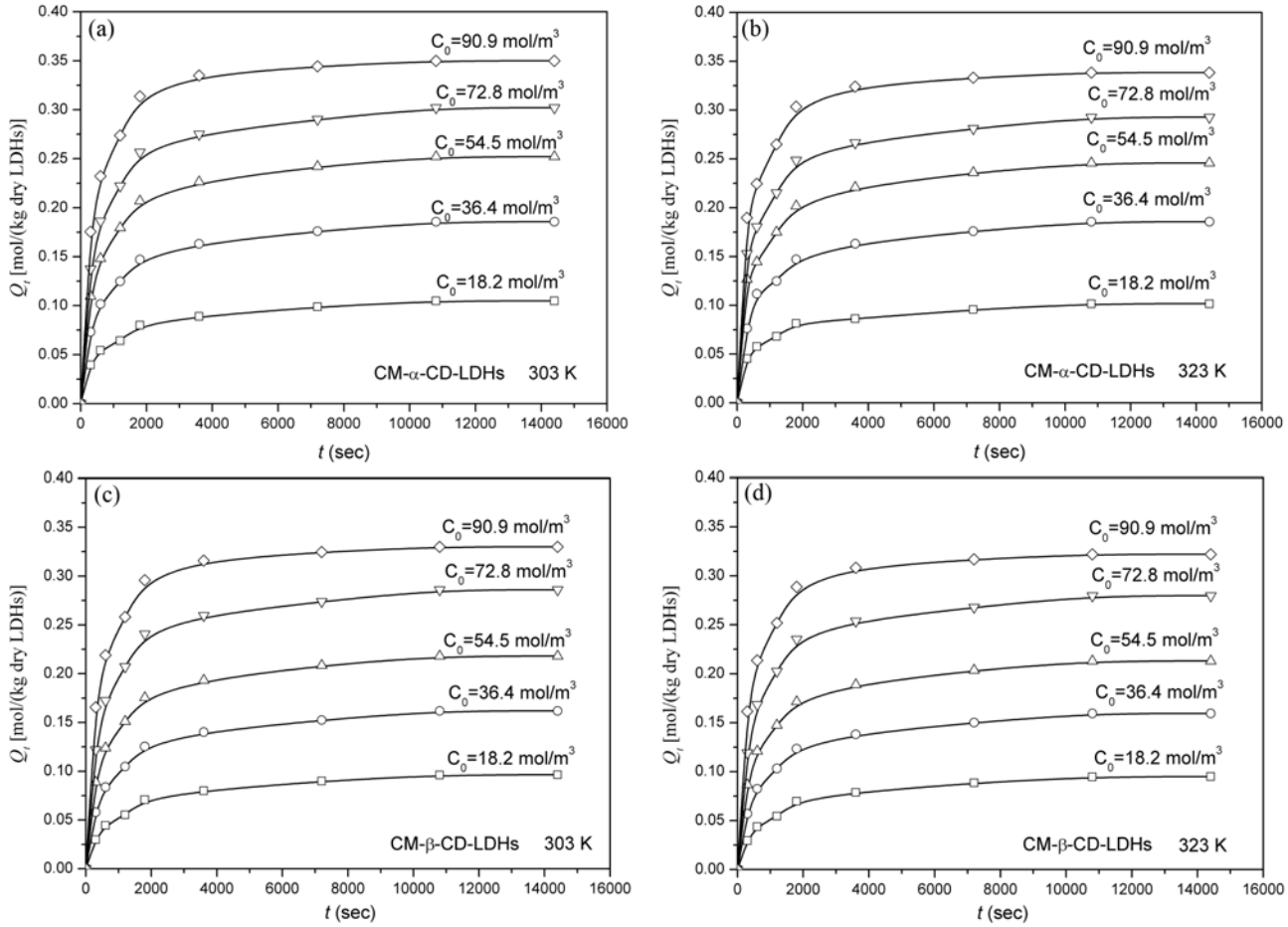

Fig. 3. Effect of concentration on the uptake curves for adsorption of Phe on (a) CM-α-CD-LDHs at 303 K, (b) CM-α-CD-LDHs at 323 K, (c) CM-β-CD-LDHs at 303 K, (d) CM-β-CD-LDHs at 323 K.

Table 3. Determined parameters against initial concentration

System	Temp. (K)	$C_{a,0}$ (mol/m^3)	$D_{eff}\times10^{-12}$ (m^2/s)	$D_c\times10^{-12}$ (m^2/s)	$D_p\times10^{-11}$ (m^2/s)	α	β
CM-α-CD-LDHs	303	18.2	3.41	1.06	5.71	22.89	0.425
		36.4	3.74			19.90	0.369
		54.5	4.05			17.76	0.330
		72.8	4.37			15.93	0.296
		90.9	4.64			14.64	0.272
	323	18.2	3.54	1.09	5.72	21.93	0.418
		36.4	3.77			19.91	0.379
		54.5	4.13			17.47	0.333
		72.8	4.51			15.43	0.294
		90.9	4.80			14.12	0.269
CM-β-CD-LDHs	303	18.2	3.66	1.19	5.74	21.75	0.451
		36.4	4.15			17.98	0.373
		54.5	4.49			16.02	0.332
		72.8	4.54			15.77	0.326
		90.9	4.83			14.45	0.299
	323	18.2	3.77	1.24	5.77	21.29	0.458
		36.4	4.25			17.73	0.381
		54.5	4.67			15.47	0.332
		72.8	4.72			15.24	0.327
		90.9	5.00			14.03	0.302

adsorbed by α-CD. As the CM-α-CD-LDHs is conveniently used and exhibits high chiral excess adsorption ratio, it can be expected that this complex has prospective application in the field of enantioselective adsorption and separation.

3. Study on the Diffusion Kinetics

In the adsorption experiments, the change of bulk concentration before and after adsorption is about 8%; as a result, the bulk concentration can be considered to be constant approximately during the adsorption process. This gives the above boundary condition at the surface of the adsorbent particle, i.e., the adsorbent-phase concentration at the surface of the particle is constant.

The value of the intraparticle effective diffusivity (D_{eff}) was determined by fitting the experimental adsorption data with Eq. (10). We initialized different values of D_{eff}, until the best fit was obtained. As shown in Fig. 3, the experimental values were well correlated by Eq. (10). The experimental values of D_{eff} are listed in Table 3. D_{eff} increased with increasing bulk-phase Phe concentration, indicating an existence of a parallel transport by both crystallite and pore diffusion in the LDHs macroparticles.

The relationship between crystallite diffusivity, pore diffusivity, and intraparticle effective diffusivity based on the parallel diffusion model is given by the following equation, which is derived from the relation between the fluxes based on the parallel diffusion model and the Fickian model:

$$D_{eff}\left[(1-\varepsilon)+\varepsilon\frac{dC}{dq}\right]=(1-\varepsilon)D_c+\varepsilon D_p\frac{dC}{dq} \tag{16}$$

In our experimental method, the adsorption isotherm could be considered linear. Therefore, the dC/dq can be approximated to C_e/q_e. Eq. (16) is transformed into Eq. (17):

$$D_{eff}\left(1+\frac{1}{\alpha}\right)=D_c+D_p\frac{1}{\alpha} \tag{17}$$

Fig. 4 shows the plot of the experimental effective diffusivities based on Eq. (17) at 303, and 323 K, respectively. The value of the intercept of the line gives the crystallites diffusivity D_c and the slope of the line provides the pore diffusivity D_p, which are listed in Table 3. The values of D_{eff}, D_c and D_p increase continuously with temperature from 303 K to 323 K, indicating that higher temperatures favor diffusion of Phe in LDHs. In all the conditions, β<0.5 (Table 3). It can be assumed that pore diffusion is the rate-controlling step.

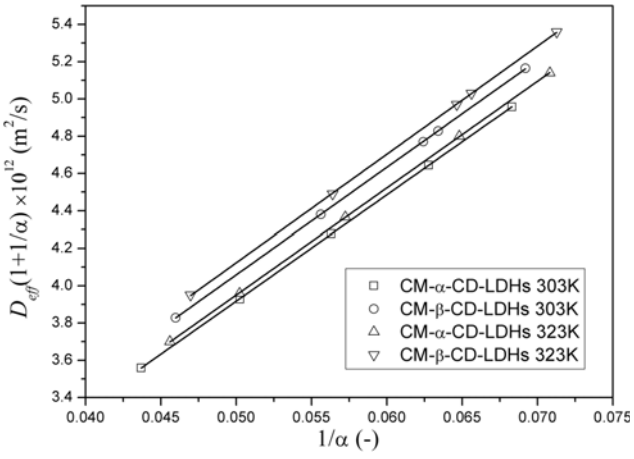

Fig. 4. Plots of intraparticle effective diffusivities based on Eq. (17).

CONCLUSIONS

The CM-α-CD-LDHs and CM-β-CD-LDHs have been demonstrated to represent chiral adsorption for (*L*,*D*)-phenylalanine. The adsorption isotherms of chiral excess adsorption as well as total adsorption of Phe by these CM-α/β-CD-LDHs have been investigated. Furthermore, the CM-α-CD-LDHs shows higher enantioselective adsorption ratio, and the increase of temperature is beneficial for chiral recognition. The parallel transport of Phe by crystallites and pore diffusion in CMCD-LDHs macroparticles was investigated. The values of the intraparticle effective diffusivity (D_{eff}) obtained from the homogeneous Fickian model and the crystallites (D_c) and pore (D_p) diffusivities were determined from the intercept and slope of the plot of $D_{eff}(1+1/\alpha)$ vs. $1/\alpha$, respectively. As the CMCD-LDHs are conveniently used and exhibit high enantioselective adsorption capacity, these CMCD functionalized inorganic layered materials may have prospective application as the basis of a novel chiral separation system.

ACKNOWLEDGEMENTS

This project was supported by the Zibo science and technology development project (Grant No.: 2011GG01156).

SYMBOLS

C : liquid-phase concentration of Phe inside the macroparticle [mol/m^3]
$C_{a,0}$: initial aqueous-phase Phe concentration [mol/m^3]
$C_{a,t}$: aqueous-phase Phe concentration at time t [mol/m^3]
$C_{a,e}$: aqueous-phase Phe concentration at equilibrium [mol/m^3]
C_{Ca} : the concentration of Ca^{2+} filled in the pore [mol/m^3]
C_e : the equilibrium concentration of Phe in the pore [mol/m^3]
$C_{f,Ca}$: the concentrate of Ca^{2+} in the filtrate [mol/m^3]
D_{eff} : intraparticle effective diffusivity [m^2/s]
D_p : pore diffusivity [m^2/s]
D_c : the effective diffusivity in the crystallites [m^2/s]
F : fractional attainment of equilibrium
m : the mass of CMCD-LDHs [kg]
q : solid-phase concentration of Phe on the surface of the crystallites microspheres [mol/m^3]
q_e : the equilibrium concentration of Phe on the adsorption sites [mol/m^3]
Q_e : $(=(1-\varepsilon)q_e+\varepsilon C_e)$ total concentration of Phe in the particle in equilibrium [mol/m^3 wet LDHs]
Q_t : $(=(1-\varepsilon)q+\varepsilon C)$ total concentration of Phe in the particle [mol/m^3 wet LDHs]
Q_{ce} : the chiral excess adsorption capacity [mol/kg]
Q_{total} : the total sorption capacity [mol/kg]
r : radial dimension of an adsorbent particle [m]
r_0 : radius of an adsorbent particle [m]
t : time [s]
V_f : the volume of the filtrate [m^3]
W : weight of the wet CMCD-LDHs particles [kg]
X : $(=C/C_e)$ dimensionless constant

Y : (=q/q_e)) dimensionless constant

Greek Letters

a : $(1-\varepsilon)q_e/\varepsilon C_e$
β : $\alpha(D_c/D_p)$
ε : void ration of LDHs macroparticles
λ_n : the nonzero roots of Eq. (16)
ξ : r/r_0
ω : final fractional uptake of solute by the LDHs macroparticles
τ_p : $D_p t/r_0^2$
τ_c : $D_c t/r_0^2$
θ : the apparent density [kg of wet CMCD-LDHs m^{-3}]

REFERENCES

1. T. H. Yoon and I. H. Kim, *Korean J. Chem. Eng.*, **21**, 521 (2004).
2. M. V. Rekharsky and Y. Inoue, *J. Am. Chem. Soc.*, **124**, 813 (2002).
3. M. Palanisamy, J. Khanam, A. Nagalingam and N. Gani, *Korean J. Chem. Eng.*, **28**, 1990 (2011).
4. K. Kano, H. Matsumoto, S. Hashimoto, M. Sisido and Y. Imanishi, *J. Am. Chem. Soc.*, **107**, 6117 (1985).
5. J. Sherma, *Anal. Chem.*, **82**, 4895 (2010).
6. P. Sun, A. Krishnan, A. Yadav, S. Singh, F. M. MacDonnell and D. W. Armstrong, *Inorg. Chem.*, **46**, 10312 (2007).
7. J. Carlstedt, A. Bilalov, E. Krivtsova, U. Olsson and B. Lindman, *Langmuir*, **28**, 2387 (2012).
8. G. R. Williams, T. G. Dunbar, A. J. Beer, A. M. Fogg and D. O'Hare, *J. Mater. Chem.*, **16**, 1231 (2006).
9. L. Jin, X. Y. Ni, X. L. Liu and M. Wei, *Chem. Eng. Technol.*, **33**, 82 (2010).
10. B. F. Sels, D. E. De Vos and P. A. Jacobs, *Angew. Chem. Int. Ed.*, **44**, 310 (2005).
11. X. Q. Hou and R. J. Kirkpatrick, *Chem. Mater.*, **14**, 1195 (2002).
12. Z. P. Xu and P. S. Braterman, *J. Phys. Chem. C*, **111**, 4021 (2007).
13. P. Sawunyama, M. Jackson and G. W. Bailey, *J. Colloid Interface Sci.*, **237**, 153 (2001).
14. H. B. Song, Z. F. Xiao and Q. P. Yuan, *J. Chromatogr. A*, **1216**, 5001 (2009).
15. L. Mohanambe and S. Vasudevan, *J. Phys. Chem. B*, **109**, 22523 (2005).
16. L. Mohanambe and S. Vasudevan, *Inorg. Chem.*, **43**, 6421 (2004).
17. X. L. Liu, M. Wei, F. Li and X. Duan, *AIChE J.*, **53**, 1591 (2007).
18. X. L. Liu, M. Wei, D. G. Evans and X. Duan, *Chem. Eng. Sci.*, **64**, 2226 (2009).
19. Y. Matsuoka, N. Kanda, Y. M. Lee and A. Higuchi, *J. Membr. Sci.*, **280** , 116 (2006).
20. H. Yoshida and W. Takatsuji, *Ind. Eng. Chem. Res.*, **39**, 1074 (2000).
21. W. A. Galinada and H. Yoshida, *AIChE J.*, **50**, 2806 (2004).
22. S. Y. Park, J. K. Park, J. H. Park, C. V. McNeff and P. W. Carr, *Microchem. J.*, **70**, 179 (2001).
23. B. J. Ravoo, R. Darcy, A. Mazzaglia, D. Nolan and K. Gaffney, *Chem. Commun.*, 827 (2001).